Int. J. Therm. Sci. (1999) 38, 937–943

Heat and mass transfer in wavy falling films of binary mixtures [1]

Stephan Leuthner, Alexander Harun Maun, Stefan Fiedler, Hein Auracher *

Institut für Energietechnik, TU Berlin, Marchstraße 18, 10587 Berlin, Germany

(Received 25 February 1999, accepted 21 April 1999)

Abstract — Heat and mass transfer in an evaporating two-component falling liquid film are considered. Based on physical phenomena of the transport processes, models for the laminar and the turbulent-wavy falling film are presented. A comparison with experimental data shows that the laminar model is only applicable for restricted conditions. Predicted heat transfer coefficients of the turbulent-wavy model are compared with data from experiments with water and water–ethylene glycol as test fluid for Reynolds numbers between 250 and 420. The model predicts well the experimental data. © 1999 Éditions scientifiques et médicales Elsevier SAS

wavy falling film / heat and mass transfer / binary mixtures / modeling / experimentation / laminar flow / turbulent flow / water / ethylene glycol / evaporation

Nomenclature

a	thermal diffusivity	$m^2 \cdot s^{-1}$
D_{AB}	diffusivity	$m^2 \cdot s^{-1}$
C	average wave velocity	$m \cdot s^{-1}$
c_p	specific heat at constant pressure	$J \cdot kg^{-1} \cdot K^{-1}$
g	gravitational constant ($= 9.8\ m \cdot s^{-2}$)	
h	film thickness	m
h_0	inlet film thickness defined by Nusselt theory	m
Δh_v	specific enthalpy of vaporization	$kJ \cdot kg^{-1}$
L	heated length	m
$L_{base\ film}$	length of the base film	m
L_{wave}	base length of the average wave	m
L_{period}	average wave separation distance	m
Le_t	turbulent Lewis number	
Nu	Nusselt number	
p	pressure	Pa
Pr_t	turbulent Prandtl number	
$\dot{q}$	heat flux	$W \cdot m^{-2}$
Re	Reynolds number	
Sc_t	turbulent Schmidt number	
u	velocity in x-direction	$m \cdot s^{-1}$
v	velocity in y-direction	$m \cdot s^{-1}$
w_τ	shear velocity	$m \cdot s^{-1}$
x	axial coordinate, in direction of gravity	m
y	y-coordinate	m
y'	dimensionless y-coordinate	

Greek symbols

α_{evap}	heat transfer coefficient	$W \cdot m^{-2} \cdot K^{-1}$
Γ	mass-flow rate per unit wetted perimeter	$kg \cdot m^{-1} \cdot s^{-1}$
δ^+	dimensionless film thickness	
δ_{wave}	mean height of wave above wall	m
$\delta_{base\ film}$	base film thickness in average wave representation	m
ε_D	turbulent mass diffusivity	$m^2 \cdot s^{-1}$
ε_H	turbulent thermal diffusivity	$m^2 \cdot s^{-1}$
ε_M	turbulent viscosity for momentum transfer	$m^2 \cdot s^{-1}$
λ	conductivity of the liquid	$W \cdot m^{-1} \cdot K^{-1}$
η	dynamic viscosity	$kg \cdot m^{-1} \cdot s^{-1}$
ν	kinematic viscosity	$m^2 \cdot s^{-1}$
ϑ	temperature	K
ρ	liquid density	$kg \cdot m^{-3}$
τ_w	wall shear stress	$N \cdot m^{-2}$

* Correspondence and reprints.
auracher@buran.fb10.tu-berlin.de

[1] This article is a follow up to a communication presented by the authors at the EUROTHERM 59 Conference, held in Nancy (France) in July 1998.

ξ'	mass fraction in the liquid mixture
ξ''	mass fraction in the vapor mixture

Subscripts

A	more volatile component
B	less volatile component
E	evaporation
en	at the entrance
H_2O	water
i	interface; inside
sat	saturation condition
wall	at the wall

1. INTRODUCTION

Falling film evaporators are increasingly used in the chemical process industry for separation of multi-component mixtures. In spite of this increasing application, little information is available on the transport processes, in particular, data and predictive models for wide-boiling mixtures, i.e. with large temperature differences between bubble and dew points, are missing [1]. For the design of falling film evaporators for single-component fluids the correlation based on investigations by Chun and Seban [2] is normally recommended in handbooks, such as VDI-Wärmeatlas [3].

Palen et al. [1] concluded that for narrow-boiling-range mixtures mass transfer effects are less important than for mixtures with a wide boiling range. Measurements of falling film evaporation by Palen et al. show that the effective heat transfer coefficients for wide-boiling-range mixtures can be as much as 80 % smaller than the ones calculated for single-component films at corresponding conditions due to a mass transfer induced elevation of the interface temperature.

At present, few models are available in the literature which account for falling film evaporation of wide-boiling-range mixtures. In the case of laminar flow without waves it is possible to derive an exact solution for the coupled momentum, mass and heat transfer in the falling film. Hoke and Chen [4] presented a solution of the mass transfer coefficient for evaporating laminar falling films without interfacial waves which enables the calculation of the heat transfer coefficients as well. Palen [5] determined experimental heat transfer coefficients for falling film evaporation of a wide-boiling-range mixture (water–ethylene glycol). He developed a semiempirical model of the coupled heat and mass transfer phenomena which permits us to predict the evaporative heat transfer coefficient with an average deviation of less than 15 %.

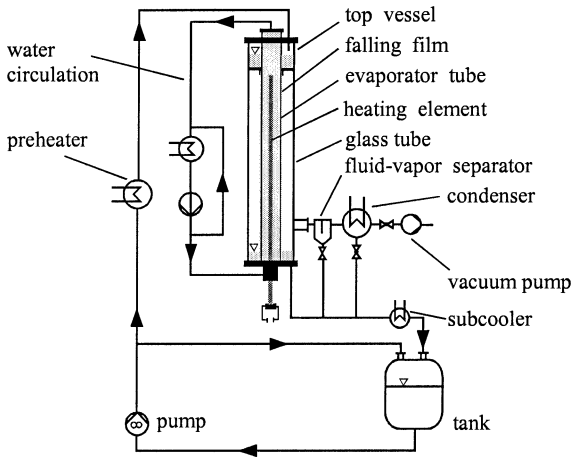

Figure 1. Schematic of the test facility.

The objective of this study is to obtain and compare predicted data from a model for laminar flow without waves with experimental data by Palen [5] for heat transfer coefficients of falling film evaporation of a wide-boiling-range mixture. Furthermore, a new model is developed for a wavy film which includes the mixing effect of waves. This model is verified by our own experimental heat transfer data.

2. EXPERIMENTAL

Figure 1 shows the test facility. It consists of an evaporator tube with 25.5 mm O.D. and 1.75 m heated length, made of copper–nickel–zinc alloy. The tube is surrounded by a glass tube of 80 mm I.D. The falling film evaporates on the tube surface. In the center of the tube an electrical heater has been installed. Water is pumped in the annulus between heater and tube, so that heat flows from the heater across the fluid to the evaporator tube. The feed solution is pumped from the tank into the top vessel of the evaporator where it is distributed uniformly onto the tube surface. The vapor formed in the evaporator is liquefied in the condenser and flows back together with the non-evaporated liquid to the tank through a subcooler.

2.1. Instrumentation

The inlet flowrate of the test fluid and the heating water flowrate are measured by turbine flowmeters. Thermocouples (Ni–CrNi) are used to measure bulk liquid temperatures at inlet and outlet of the evaporator tube and in

the vapor space (accuracy: 0.1 K). The heating water temperature is measured before and after the heating section. Thermocouples have been inserted into slots in the evaporator tube at different lengths to measure local temperatures. The heating power of the cartridge heater is determined by a power meter and the vapor space pressure in the evaporator by a manometer. Tests were run with water and a water–ethylene glycol mixture (mass fraction of water: $\xi'_{H_2O} = 0.87$–0.90). The concentration of ethylene glycol in the feed was analyzed by a gas chromatograph.

The inlet Reynolds numbers were in the range between 230 and 420, and the evaporative heat flux was varied from 14 to 19 kW·m^{-2}. For the mixture the evaporation heat flux had to be decreased to 4–5 kW·m^{-2} to avoid nucleate boiling at Reynolds numbers larger than 270. The fluid subcooling was approximately 3–8 K at the inlet. The system pressure varied from 4700 to 6300 Pa.

2.2. Data evaluation

The heat flux at the outer tube surface is determined numerically by solving the energy and momentum equations for the annulus space between cartridge heater and inner tube diameter. The solution includes the subcooled region just downstream of the liquid distributor. Input data for the numerical solution are the power of the cartridge heater inside the tube and the temperature at the inner tube wall, measured by thermocouples. Local temperatures (υ_{wall}) at the outer diameter of the tube are obtained. The heat transfer coefficient of the falling film is then calculated as:

$$\alpha_{evap} = \dot{q}/(\upsilon_{wall} - \upsilon_{sat}) \tag{1}$$

where υ_{sat} is the film surface temperature, which is measured by thermocouples at the interphase. Hence, local heat transfer coefficients are obtained in contrast to an earlier study [6] where only average quantities have been determined. From an error analysis the uncertainty in the resulting heat transfer coefficient was determined to be 10 %. For the low heat fluxes the uncertainty is 11 %.

3. MODELING

In falling films different flow conditions are encountered. At small flow rates the film is smooth and can be assumed to be laminar. At higher flow rates the film becomes wavy with increasing distance from the inlet. The flow pattern can be subdivided in a smooth entrance section of the length L_{en} and downstream of this region in a wavy section (*figure 2A*). According to Brauner and Maron [7] L_{en} depends on the Nusselt film thickness h_0 and the film Reynolds number $Re = \Gamma/\eta$:

$$\text{for } Re \le 125, \quad L_{en} = 500 h_0 \tag{2}$$

$$\text{for } Re > 125, \quad L_{en} = (350 + 0.12\,Re) h_0 \tag{3}$$

Telles and Dukler [8] have shown that the wavy film structure consists essentially of two portions, a thin base film portion flowing next to the wall and thick turbulent waves. In our model the base film is assumed to be laminar. For the waves a turbulent model including an eddy–diffusivity profile is applied.

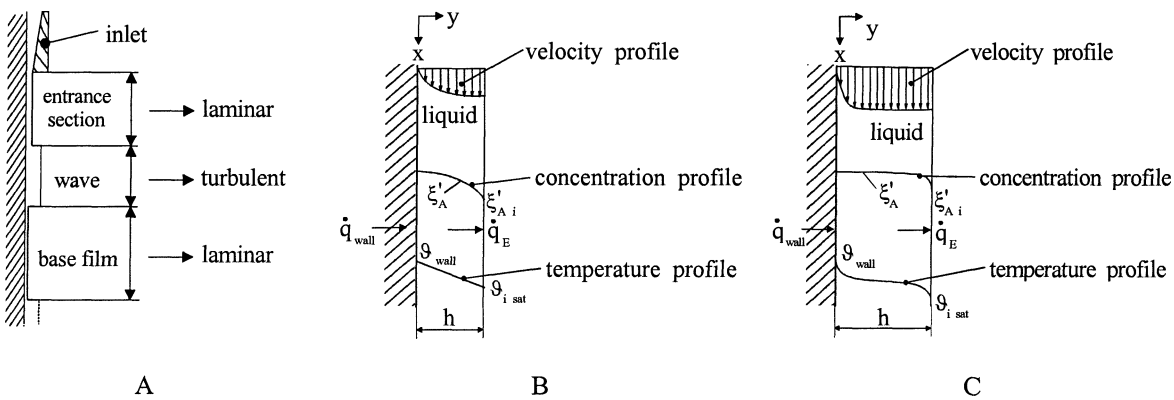

Figure 2. Different sections of a wavy falling film (A); concentration, temperature and velocity profiles in a laminar (B) and a turbulent (C) falling liquid film of a mixture.

Falling film evaporation of a wide-boiling-range binary mixture is considered for the laminar and turbulent region. In the case of surface evaporation all the heat flux leaving the solid wall and passing through the liquid film serves to evaporate the liquid at the interface. The more volatile component A is preferentially evaporated, causing a decrease in the local concentration of this component. This process results in a convex local concentration profile as indicated in *figures 2B* and *2C*, with maximum concentration of A at the wall and minimum concentration at the interface ξ'_{Ai}. Moving in axial direction, the concentration at the interface ξ'_{Ai} decreases and the corresponding evaporation temperature $\upsilon_{i\ sat}$ increases.

3.1. Physical model for a smooth laminar film

For the laminar model the governing equations for continuity, momentum, component continuity and energy [equations (4)–(8)] have been solved numerically using finite differences. The assumptions made are described in [6]. Coordinates are defined in *figure 2*, u denotes the velocity in x-direction, v the velocity in y-direction. In the momentum equation (5) v is not included since a Nusselt profile is always assumed and the v-component of the velocity follows from the continuity equation (4).

$$\frac{\partial u}{\partial x} + \frac{\partial v}{\partial y} = 0 \tag{4}$$

$$\eta \frac{\partial^2 u}{\partial y^2} = -\rho g \tag{5}$$

$$\frac{\partial p}{\partial y} = 0 \tag{6}$$

$$u\frac{\partial \xi'_A}{\partial x} + v\frac{\partial \xi'_A}{\partial y} = D_{AB}\frac{\partial^2 \xi'_A}{\partial y^2} \tag{7}$$

$$\rho c_p\left(u\frac{\partial \upsilon}{\partial x} + v\frac{\partial \upsilon}{\partial y}\right) = \lambda\frac{\partial^2 \upsilon}{\partial y^2} \tag{8}$$

Three boundary conditions are required to obtain a solution of equation (7):

$$x = 0; \quad \xi'_A = \xi'_{A0}$$

$$y = 0; \quad \frac{\partial \xi'_A}{\partial y} = 0$$

$$y = h; \quad \frac{\partial \xi'_A}{\partial y} = \frac{\dot{q}_E g(\xi'_{Ai} - \xi''_{Ai})}{\rho D_{AB}[\xi''_{Ai}(\Delta h_{vA} - \Delta h_{vB}) + \Delta h_{vB}]}$$

The boundary condition for $y = h$ was derived by an energy and mass balance at the interface, the vapor phase resistance was taken to be negligible [4]. Also three boundary conditions are required to obtain a solution of equation (8):

$$x = 0; \quad \upsilon = \upsilon_{sat}(\xi'_{A0})$$

$$y = 0; \quad \frac{\partial \upsilon}{\partial y} = -\frac{\dot{q}_w}{\lambda}$$

$$y = h; \quad \upsilon = \upsilon_{sat}(\xi'(h))$$

The heat and mass transfer equations are coupled through the boundary condition for $y = h$ and through the evaporative heat flux $\dot{q}_E$ at the interface. $\dot{q}_E$ follows from the temperature gradient at the interface by $\dot{q}_E = -\lambda(\partial\upsilon/\partial y)$. This model for a smooth laminar film was applied in the entrance section and in the base film sections.

3.2. Physical model for a wavy liquid film

The turbulent model for the waves is based on recent experimental information on the physical structure of wavy liquid films. The waves carry a significant fraction of the total flow and move independently of each other over the base film with no change in speed or shape [9]. Telles and Dukler determined wave parameters which characterize this structure for liquid Reynolds numbers from 250 up to about 2500. These wave parameters are δ_{wave} (average height of wave above wall), $\delta_{base\ film}$ (base film thickness in average wave representation), L_{wave} (average base length of the wave), L_{period} (average wave separation distance), and C (average wave velocity) (*figure 3*).

The momentum, component continuity and energy equations for the thick turbulent waves are given below. u denotes the steady state component of the turbulent flow velocity.

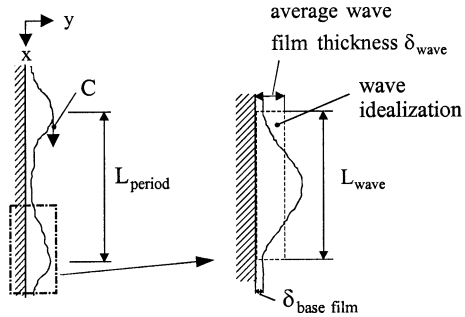

Figure 3. Representation of wavy film characteristics.

$$\frac{\mathrm{d}}{\mathrm{d}y}\left((\nu+\varepsilon_{\mathrm{M}})\frac{\mathrm{d}u}{\mathrm{d}y}\right)+g=0 \tag{9}$$

$$u(y)\frac{\partial \xi'_{\mathrm{A}}}{\partial x}=\frac{\partial}{\partial y}\left((D_{\mathrm{AB}}+\varepsilon_{\mathrm{D}})\frac{\partial \xi'_{\mathrm{A}}}{\partial y}\right) \tag{10}$$

$$u(y)\frac{\partial \upsilon}{\partial x}=\frac{\partial}{\partial y}\left((a+\varepsilon_{\mathrm{H}})\frac{\partial \upsilon}{\partial y}\right) \tag{11}$$

Two boundary conditions are required to obtain a solution of equation (9):

$$y=h:\quad \frac{\mathrm{d}u}{\mathrm{d}y}=0; \qquad y=0:\quad u=0$$

For the component continuity and the energy equation the same boundary conditions as for the smooth laminar film have been used; for further assumptions see [6]. The effect of turbulent eddies is taken into account by introducing the turbulent transport coefficients ε_{M}, ε_{D} and ε_{H}. As the turbulent Lewis number $Le_{\mathrm{t}}=Sc_{\mathrm{t}}/Pr_{\mathrm{t}}$ is assumed to be unity and the turbulent Prandtl number $Pr_{\mathrm{t}}=\varepsilon_{\mathrm{M}}/\varepsilon_{\mathrm{H}}$ is taken to be 0.9, the turbulent thermal diffusivity ε_{H} and the turbulent mass diffusivity ε_{D} have the same value: $\varepsilon_{\mathrm{H}}=\varepsilon_{\mathrm{D}}=\varepsilon_{\mathrm{M}}/0.9$. For the turbulent viscosity, a modified van Driest profile proposed by Grabbert [10] was applied:

$$\frac{\varepsilon_{\mathrm{M}}}{\nu}=\frac{1}{2}\Bigg[1+0.64\left(\delta^{+}y'\sqrt{1-y'}\right)^{2}\cdot\left(1-\exp\left(-\frac{\delta^{+}y'\sqrt{1-y'}}{26}\right)\right)^{2}\Bigg]^{1/2}-\frac{1}{2} \tag{12}$$

where $y'=y/h_0$ is a dimensionless y-coordinate and δ^{+} is the dimensionless film thickness. $w_\tau=\sqrt{\tau_{\mathrm{w}}/\rho}$ denotes the shear velocity, τ_{w} is the shear stress at the wall. The wave parameters have been adapted to the mixture in the same manner as proposed by Brumfield and Theofanous [9], based on the different Prandtl number of the mixture.

As mentioned above, the governing equations are solved numerically using finite differences. Therefore start profiles for concentration and temperature in the wave and in the base film are required. They are determined using the profiles at the end of the laminar entrance section (see *figure 2A*). For the start profiles of the wave at $x=L_{\mathrm{en}}$, the profiles in the film at the end of the entrance section are taken over directly up to the base film thickness, which is smaller than the thickness of the film in the entrance section. In the portion between $\delta_{\mathrm{base\ film}}$ and δ_{wave} the profiles of the remaining part ($\delta_{\mathrm{en}}-\delta_{\mathrm{base\ film}}$) are stretched linear. For the start profiles of the base film the profiles are taken over directly from the end of the entrance section. With the start profiles established, the temperature and concentration fields are calculated at turbulent conditions for the wave length L_{wave} and at laminar conditions for the length of the base film $L_{\mathrm{base\ film}}$, as depicted in *figure 4*.

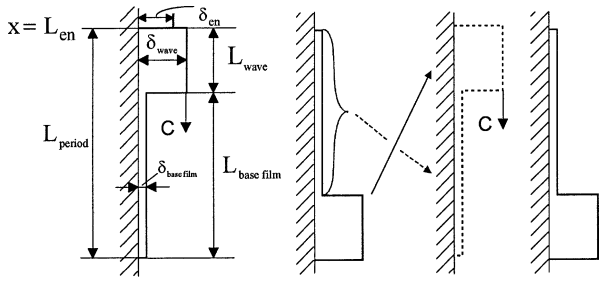

Figure 4. Illustration of wave model procedure.

Subsequently, a turbulent wave moves over the laminar base film with the average wave velocity C (*figure 4*) which is much higher than the velocity of the base film. The wave continuously incorporates the concentration and temperature profiles of the base film found in front of it and at the tail the concentration and temperature profiles of the wave form the new profiles in the base film left behind. Once the wave reaches the end of one base film section, the subsequent concentration or temperature profiles of the base film are not known *a priori*. Therefore an iterative process is employed: the base film which is left after one wave has completely moved over it is placed now in front of the wave. Then the wave moves over it until reaching the end of this base film, leading to new concentration and temperature profiles in the base film. In contrast, the profiles in the wave are kept constant. This procedure is repeated until the mean heat transfer coefficient of this wave period remains constant. Then the entire procedure is repeated for each subsequent wave period until the end of the evaporator tube is reached. A mean heat transfer coefficient and hence a mean Nusselt number can be calculated for the entire falling film including the wavy section and the laminar entrance section.

4. RESULTS AND DISCUSSION

4.1. Comparison of experimental data with predicted data from the laminar model

Palen [5] carried out experiments on evaporation of water–ethylene glycol mixtures inside a vertical tube.

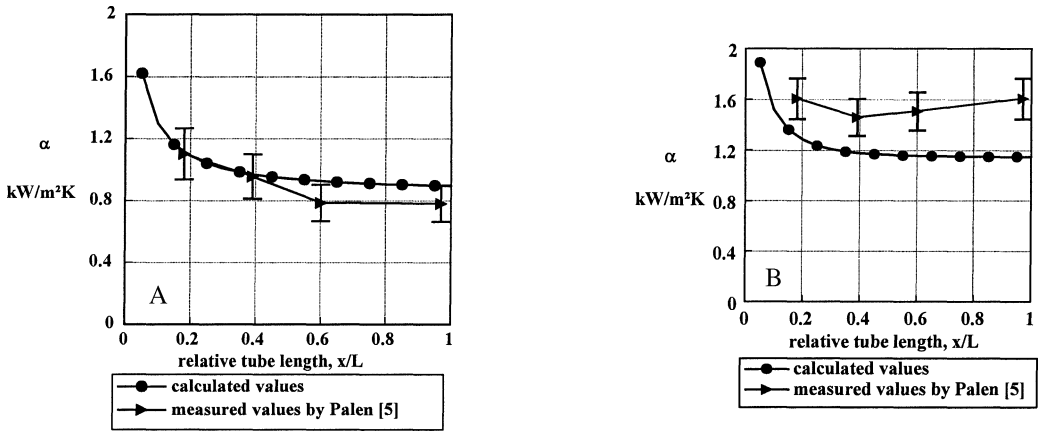

Figure 5. Heat transfer coefficient versus tube length, A: $\xi'_{H_2O} = 0.11$, $p = 100$ kPa, $L = 1.45$ m, $Re = 275$; B: $\xi'_{H_2O} = 0.35$, $p = 100$ kPa; $L = 1.45$ m, $Re = 225$.

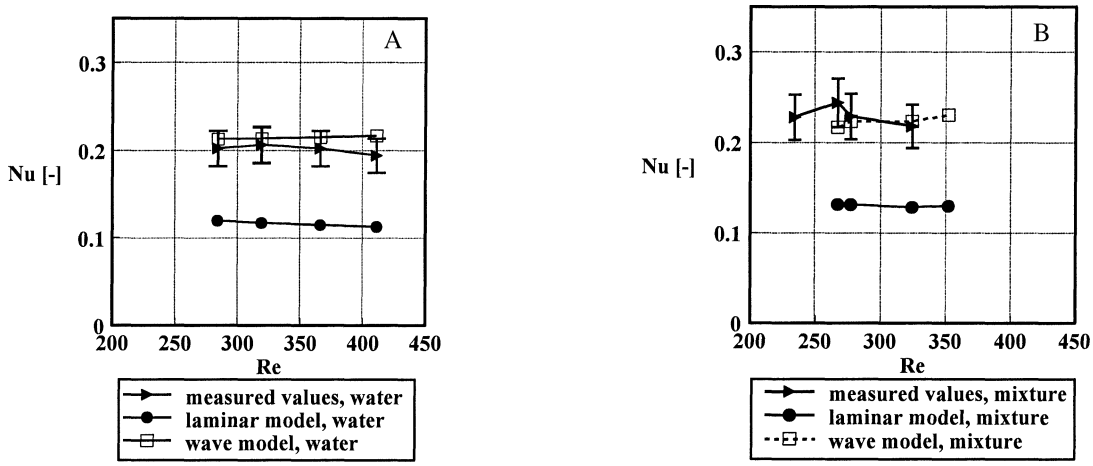

Figure 6. Average Nusselt number versus film Reynolds number for the falling film evaporation of water (case A) and a water–ethylene glycol mixture (case B) (water mass fraction: $\xi'_{H_2O} = 0.87$–0.9).

Figure 5 shows the heat transfer coefficient versus the tube length in comparison with our predicted data from laminar modeling.

For a mass fraction of about 0.11 at $Re = 275$ (case A), nearly all of the predicted data lie within the error limits of the measured heat transfer coefficients. However, with an increasing water inlet concentration, the absolute deviation increases even with decreasing *Re* numbers. For a water mass fraction of 0.35 at $Re = 225$ (case B), e.g., the predicted data lie outside of the error limits. Obviously, the limit of laminar behavior is determined by both the water concentration and the *Re* number. It is quite likely that due to the different fluid properties in case B the film becomes wavy even at smaller Reynolds numbers than in case A. At present experiments are being carried out to quantify these limits.

4.2. Comparison of experimental data with predicted data from the wavy film model

To compare heat transfer coefficients of falling films at different temperatures and of different fluids, the Nusselt number is used:

$$Nu = \frac{\alpha}{\lambda}\left(\frac{\nu^2}{g}\right)^{1/3} \tag{13}$$

Figure 6 shows the *Nu* number versus the *Re* number (based on the flow rate at the inlet at saturation temperature) of our measured data in comparison with the predicted ones for pure water (case A) and a mixture (case B). The calculations have been carried out for pressures and heat fluxes corresponding to the experimental conditions and a tube length of 1.75 m.

The accuracy of the wave model for the case of water shows a very good approach compared with the measured values (*figure 6A*). The deviation according to the wave model for the case of the mixture is also reasonably good. On the contrary, the heat transfer coefficients predicted by the laminar model are significantly smaller than the experimental data.

The objectives of future studies are to obtain quantitative information about the wave patterns for Reynolds numbers smaller than 250 for water and mixtures.

5. CONCLUSION

Heat and mass transfer of an evaporating wavy falling film of a water–ethylene glycol mixture can be predicted by a numerical procedure, including flow, temperature and concentration field. The model includes wave parameters from the literature. The accuracy of the prediction compared with measurements is reasonably good at Reynolds numbers above 250. In future investigations information about the wave parameters at Reynolds numbers smaller than 250 will be determined experimentally to apply the model at $Re < 250$ as well.

Acknowledgements

We would like to acknowledge the financial support by the EU (JOULE II-project) and the help of M. Habijan. The authors also thank Wieland-Werke AG for the test section.

REFERENCES

[1] Palen J.W., Wang Q., Chen J.C., Falling film evaporation of binary mixtures, AIChE J. 40 (2) (1994) 207–214.

[2] Chun K.R., Seban R.A., Heat transfer to evaporating liquid films, J. Heat Trans.–T. ASME 93 (1971) 391–396.

[3] VDI-Wärmeatlas (VDI Heat Handbook), 8th Ed., VDI-Verlag, Berlin, 1997.

[4] Hoke B.C. Jr., Chen J.C., Mass transfer in evaporating falling liquid film mixtures, AIChE J. 38 (5) (1992) 781–786.

[5] Palen J.W., Falling film evaporation of wide-boiling-range mixtures inside a vertical tube, PhD. Thesis, Lehigh University, 1988.

[6] Leuthner S., Fiedler S., Auracher H., Modeling of heat and mass transfer in falling films of binary mixtures and experimental verification, in: Proc. 15th UIT National Heat Transfer Conference, Italy, ETS, Pisa, 1997, pp. 639–650.

[7] Brauner N., Maron D.M., Characteristics of inclined thin films, waviness and the associated mass transfer, Int. J. Heat Mass Tran. 25 (1) (1982) 99–110.

[8] Telles A.S., Dukler A.E., Statistical characteristics of thin, vertical, wavy, liquid films, Ind. Eng. Chem. Fundam. 9 (3) (1970) 412–421.

[9] Brumfield L.K., Theofanous T.G., On the prediction of heat transfer across turbulent liquid films, J. Heat Trans.–T. ASME 98 (3) (1976) 496–502.

[10] Grabbert G., Modellvorstellungen zum Impulstransport in Rieselfilmen, Freiberger Forschungshefte, Deutscher Verlag f. Grundstoffindustrie, Freiberg, 1990, A 806.